Proceedings of the SPIE Conference on Polarization: Measurement, Analysis, and Remote Sensing VI April 2004

Stokes Vector Component Versus Elementary Factor Performance in a Target Detection Algorithm

Frank Crosby
Naval Surface Warfare Center, Dahlgren Division, Panama City, Florida

ABSTRACT

Polarization based detection is often accomplished by using two separate components, reflectivity/emissivity and polarization, as detection algorithm inputs. These are Stokes vector components and are derived from elementary factors that represent energy collected with different polarizers. The elementary factors are added to produce the reflectivity/emissivity component and subtracted to produce the polarization component. Using the reflectivity/emissivity and polarization clearly addresses the advantage of using polarization as an added discriminant. However, depending on the detection algorithm, it may be better to use the elementary factors as input into a detection algorithm. A constant false alarm rate detection algorithm derived from a maximum likelihood is used as a foundation for judging target detection with these two different inputs. The results are presented for detecting man-made objects on natural backgrounds. The data covers is from sunlight illuminated scenes. Detection using the elementary factors is shown to be consistent with detection using the Stokes vector components and is shown to decrease the false alarm rate.

1. INTRODUCTION

Polarization is typically and added discriminant to a baseline electro-optical detection system. For program managers who must often justify the addition of polarization, the advantages are often demonstrated by applying a detection algorithm to two sets of images. One set contains no polarization information; the other set is the same as the first set with the addition of an image that only contains polarization contrast. A direct comparison can then be made between the two results.

Polarization can be completely described with the four Stokes parameters. They are commonly used since their elements are simply constructed from measurable quantities. These quantities are collected to form elementary factor images. The elementary factors can be combined in Stokes components which, not only to characterize polarization, but also reflectivity/emissivity. However, computing the Stokes components does not add information content to the original data. Therefore, an investigation into the effectiveness of detection using the elementary factors images is in order.

Computing the Stokes components requires image calibration, additional data manipulation, and is may be more susceptible to numerical errors. Achieving similar detection capabilities without the additional steps will be shown to have significant advantages. This paper will show that combining two elementary factor images directly into a detection algorithm provides effective, efficient, and more robust detection capabilities when detecting objects on a non-polarizing background. The definitions of different elementary factor images is covered in Section 2. Section 2 also discusses polarization in terms of Stokes parameters. The calculation of degree of polarization images and the reflectivity/emissivity images are also discussed.

The multi-dimensional constant false alarm rate detector is briefly reviewed in Section 3. The detection algorithm exploits geometric target features and contrast differences between targets and their surrounding areas. The detection algorithm is derived from a general statistical model of the data with the greatest emphasis on the background.

The comparison between the two approaches to target detection is given in Section 4. Theoretically, the detection approaches are shown to be consistent. That is, that detection in either case leads to detection in the other case. Further, using the elementary factor images results in a lower or equal false alarm rate compared to using the derived Stokes components: polarization and reflectivity/emissivity. Section 5 presents the results of processing some polarization data. The imagery is of spectrally low-contrast man-made objects on a variety of natural backgrounds. These examples demonstrate the theoretical prediction of Section 4.

2. DEGREE OF POLARIZATION

2.1. Polarization

Polarization can be completely described with the four Stokes parameters. They are commonly used since their elements are simply constructed from measurable components. The first parameter is the total intensity of the light and contains no polarization information. The second is the amount of linear polarization, both parallel and perpendicular. The third parameter is the amount of linear polarization oriented at either a 45° or -45°. The forth is the amount of circular polarization.

The Stokes parameters may be written as a vector:

$$\mathbf{S} = \begin{pmatrix} S_0 \\ S_1 \\ S_2 \\ S_3 \end{pmatrix}.$$

The Stokes parameters may be constructed by collecting four elementary factor images, each measuring light intensities through a differently oriented polarizer or retarder. The images are: $I(0°,0)$, which is an image collected using a linear polarizer oriented at 0°; $I(90°,0)$ an image collected using a linear polarizer oriented at 90°; $I(45°,0)$, an image collected using a linear polarizer oriented at 45°; and $I(45°,\pi/2)$, an image collected using a linear polarizer oriented at 45° along with a ¼ wave-plate retarder.

The Stokes parameters are related to these measurements by

$$\begin{aligned} S_0 &= I(0°,0) + I(90°,0) \\ S_1 &= I(0°,0) - I(90°,0) \\ S_2 &= 2I(45°,0) - s_0 \\ S_3 &= S_0 - 2I\left(45°,\pi/2\right). \end{aligned}$$

The degree of polarization is a measure of the portion of polarized light relative to the total intensity. In terms of the Stokes parameters, the degree of polarization is

$$\mathrm{DOP} = \frac{I_{\mathrm{pol}}}{I_{\mathrm{tot}}} = \frac{\sqrt{S_1^2 + S_2^2 + S_3^2}}{S_0}.$$

Target detection algorithms for landmines have focused on the degree of linear polarization (DOLP) [1,2,3]. It is common in these applications to denote $I(0°,0)$ by *P*, for parallel, and $I(90°,0)$ by *S*, German for perpendicular. Using this notation

$$\mathrm{DOLP} = \frac{|S_1|}{S_0} = \frac{|P-S|}{P+S}$$

3. CONSTANT FALSE ALARM RATE DETECTOR

A maximum likelihood ratio test generalized to two dimensions and adapted for image applications was chosen for this application[4]. It is an adaptive constant false alarm rate technique that uses spatial and spectral information. It requires few initial assumptions about the data. The algorithm was developed from the observation that many images with ground resolution of a few inches can be locally modeled with Gaussian distributions and that targets and background have a similar covariance.

The algorithm is a scalar-valued function of three 2-dimensional quantities: average target intensity, average background intensity, and common covariance of the background and target. In these polarization and reflectivity/emissivity each pixel

is a 2-dimensional sample that can be represented by the column vector $\mathbf{x}_i = [x_1, x_2]^{\mathrm{T}}$. When the sample comes from $P-S$ and $P+S$, $\mathbf{x}_i = [x_{P-S}, x_{P+S}]^{\mathrm{T}}$; for *P* and *S*, $\mathbf{x}_i = [x_P, x_S]^{\mathrm{T}}$.

A local sample of the image of size *N* is given by the $2 \times N$ matrix $\mathbf{X} = [\mathbf{x}_1 \cdots \mathbf{x}_N]$. This sample is divided into three disjoint pixel sets, background pixels, $\mathbf{B} = [\mathbf{b}_1, \ldots, \mathbf{b}_{N_\mathbf{B}}]$, possible target pixels, $\mathbf{T} = [\mathbf{t}_1, \ldots, \mathbf{t}_{N_\mathbf{T}}]$, and guard band pixels that likely contain both target and background contributions. The guard band pixels are not used in the detection metric calculation. The average target intensity, average background intensity, and common covariance of the background and target are estimated from the sample.

The mean of the target pixels is given by the 2-dimensional vector $\sum_{N_\mathbf{T}} \mathbf{t} \Big/ N_\mathbf{T} = \mu_\mathbf{T}$. The mean of the background is given by the *p*-dimensional vector $\sum_{N_\mathbf{B}} \mathbf{b} \Big/ N_\mathbf{B} = \mu_\mathbf{B}$. Let $\bar{\mathbf{b}}$ be a vector of the same length as **B** each element of which is identical and equal to $\mu_\mathbf{B}$ and $\bar{\mathbf{t}}$ be a vector of the same length as **T** each element of which is identical and equal to $\mu_\mathbf{T}$. These vectors can be used to compute the common covariance matrix:

$$\mathbf{S} = \frac{1}{N-2}\left[(\mathbf{B}-\bar{\mathbf{b}})(\mathbf{B}-\bar{\mathbf{b}})^{\mathrm{T}} + (\mathbf{T}-\bar{\mathbf{t}})(\mathbf{T}-\bar{\mathbf{t}})^{\mathrm{T}}\right].$$

The detection metric is a quadratic form and calculated as

$$F(\mathbf{X}) = \frac{N_\mathbf{B} N_\mathbf{T}}{N}(\mu_\mathbf{B} - \mu_\mathbf{T})^{\mathrm{T}} \mathbf{S}^{-1} (\mu_\mathbf{B} - \mu_\mathbf{T}).$$

Applying the $F(\mathbf{X})$ detection metric to the images $P-S$ and $P+S$ will be denoted by $F(P-S, P+S)$ and similarly, applying it to *P* and *S* will be denoted by $F(P, S)$.

Based on an initial assumption of Gaussian statistics, the probability distribution of false alarms follows an F distribution that depends on the number of dimensions and the cumulative sizes of the target and background masks[4]. It is independent of the actual or estimated background and target distributions. If the desired probability of a false alarm is α, then

$$\alpha = 1 - F_{0,\,2,\,N-3}\left(\left(\frac{N-3}{2}\right)\left(k^{\frac{-2}{N}} - 1\right)\right),$$

where $F_{0,\,2,\,N-3}$ denotes a central F-distribution (the 0 indicates a zero centrality parameter) with 2 and $N-3$ degrees of freedom. The number *k* is the threshold for the detection metric. As α decreases, the threshold increases. So, for a given sample, a higher detection value corresponds to a lower probability the sample is a false alarm.

4. COMPARISON

Clearly, the first criterion is consistency. Neither approach should introduce unique detections nor miss objects that could be detected in the other approach. Further, inputting the elementary factor images should not increase the false alarm rate compared to inputting a reflectivity/emissivity and polarization image.

4.1. Consistency

A detection value obtained using the polarization only and reflectivity/emissivity images in the detection algorithm, $F(P-S, P+S)$, and the linear polarization images, $F(P,S)$ are consistent if $F(P-S, P+S) \neq 0 \Leftrightarrow F(P,S) \neq 0$

If $F(P,S) \neq 0$, then there is either a polarization difference or a reflectivity/emissivity difference. This means that $\mu_{\mathbf{B}}^{P} - \mu_{\mathbf{T}}^{P} \neq 0$ or $\mu_{\mathbf{B}}^{S} - \mu_{\mathbf{T}}^{S} \neq 0$. Obviously, then

$$\begin{bmatrix} (\mu_{\mathbf{B}}^{P-S} - \mu_{\mathbf{T}}^{P-S}) \\ (\mu_{\mathbf{B}}^{P+S} - \mu_{\mathbf{T}}^{P+S}) \end{bmatrix} \neq \begin{bmatrix} 0 \\ 0 \end{bmatrix}$$

and so, $F(P-S, P+S) \neq 0$.

If $F(P-S, P+S) \neq 0$, then either there is a polarization difference between the target and the background or there is a reflectivity/emissivity difference.

Pure reflectivity/emissivity differences are manifest in the $P+S$ image. Pure polarization differences are present in the difference image. If there is a polarization difference between the target and the background, then there must be an intensity difference in *P* or *S*, so that either $\mu_B^P - \mu_T^P \neq 0$ or $\mu_B^S - \mu_T^S \neq 0$. Thus,

$$F(P,S) = \begin{pmatrix} \mu_B^P - \mu_T^P \\ \mu_B^S - \mu_T^S \end{pmatrix}^T \left[\mathbf{S}_{P,S}\right]^{-1} \begin{pmatrix} \mu_B^P - \mu_T^P \\ \mu_B^S - \mu_T^S \end{pmatrix} \neq 0,$$

since the covariance, **S,** is positive definite.

Similarly, if there is a reflectivity/emissivity difference between target and background, then the above equation still holds. Combining the results, $F(P,S) \neq 0$.

4.2. False Alarm Rate

Each of the two detection metrics, $F(P,S)$ and $F(P-S, P+S)$, have the same number of dimensions, $p = 2$, and the target and background sample sizes are unchanged. Since the false alarm distribution only depends on these two factors, the false alarms are identically distributed. Therefore, a direct comparison of detection values is justified. Given identical samples, if the two metrics give the same detection values, then no advantage is realized. In general, a higher detection value corresponds to a lower probability that a sample is a false alarm. Therefore, consistently higher values in one of the applications are equivalent to a theoretically lower false alarm rate.

The comparison of $F(P,S)$ to $F(P-S, P+S)$ can be demonstrated by the difference $F(P,S) - F(P-S, P+S)$. The covariance of this difference shows its behavior as a quadratic form. If it can be shown that the covariance of the difference is positive semidefinite, then $F(P,S)$ will have a lower or equal false alarm rate than $F(P-S, P+S)$.

The independence of reflectivity/emissivity and polarization means that the off-diagonal elements of the covariance of $F(P-S, P+S)$ are zero. This simple matrix form and the relation

$$\begin{bmatrix} (\mu_{\mathbf{B}}^{P-S} - \mu_{\mathbf{T}}^{P-S}) \\ (\mu_{\mathbf{B}}^{P+S} - \mu_{\mathbf{T}}^{P+S}) \end{bmatrix} = \begin{bmatrix} (\mu_{\mathbf{B}}^{P} - \mu_{\mathbf{B}}^{S} - (\mu_{\mathbf{T}}^{P} - \mu_{\mathbf{T}}^{S})) \\ (\mu_{\mathbf{B}}^{P} + \mu_{\mathbf{B}}^{S} - (\mu_{\mathbf{T}}^{P} + \mu_{\mathbf{T}}^{S})) \end{bmatrix}$$

can be used to simplify the difference formula.

The properties of the covariance matrix of the difference depend on three factors, var(P), var(S) and cov(P,S). The dimension, $p = 2$, gives a 2 x 2 matrix that prevents a unique solution for more than two variables. To simplify this underdetermined system, only the most common detection problem is addressed. That problem is detecting objects in natural backgrounds. Most natural backgrounds reflect unpolarized light regardless of the polarization of the incident illumination. Thus, we assume $P = S$ and in particular, var(P) = var(S). While the covariance term, **S**, is a function of both the target and the background, the background usually has a much larger sample size than the target and dominates the behavior.

The covariance matrix of the difference is positive semidefinite since it can be shown that all of the principal submatrices have nonnegative determinants. Thus, $F(P,S) \geq F(P-S,P+S)$. Therefore, $F(P,S)$ has a lower or equal false alarm rate than $F(P-S,P+S)$.

5. EXPERIMENTAL RESULTS

The experimental investigations demonstrate the validity of the initial assumptions of the maximum likelihood ratio test, the additional constraint used in the false alarm rate comparison, and illustrate a lower false alarm rate for the directly measured data. The initial assumptions of the maximum likelihood test are Gaussian distributions for both the target and background. These conditions lead to a false alarm frequency that follows an F-distribution. The additional condition used in the comparison of the false alarm rates of the directly measured data versus the derived data is that natural backgrounds tend to depolarize light resulting in equal distributions, or at least equal variances, between the parallel and perpendicular receivers.

5.1. Sunlight Source

This data was collected using a Tunable Filter Multispectral Camera. The camera has three channels, each with liquid crystal tunable filter (LCTF) that has 128 different selectable wavelength settings. Together, the channels cover wavelengths from 375 nm to 900 nm. Each LCTF has a preferred polarization state that it transmits best of all. There is an additional stage in front of the filter that prepares the incoming polarization by inducing up to a wavelength of retardance on it[5]. Thus, it can change the polarization of the light to which the camera is most sensitive from vertical to circular to horizontal to circular of opposite helicity, and back then to vertical. A full discussion of the sensor and the data collected is available in reference no. 6.

Figure 1 is a dual histogram formed with parallel and perpendicular (relative to the plane of incidence) polarization receivers. The sample is of a grass background and the size is over 10,000 points. The data shows that both histograms are similar and may be represented by a Gaussian distribution. The receiver output is calibrated digital count.

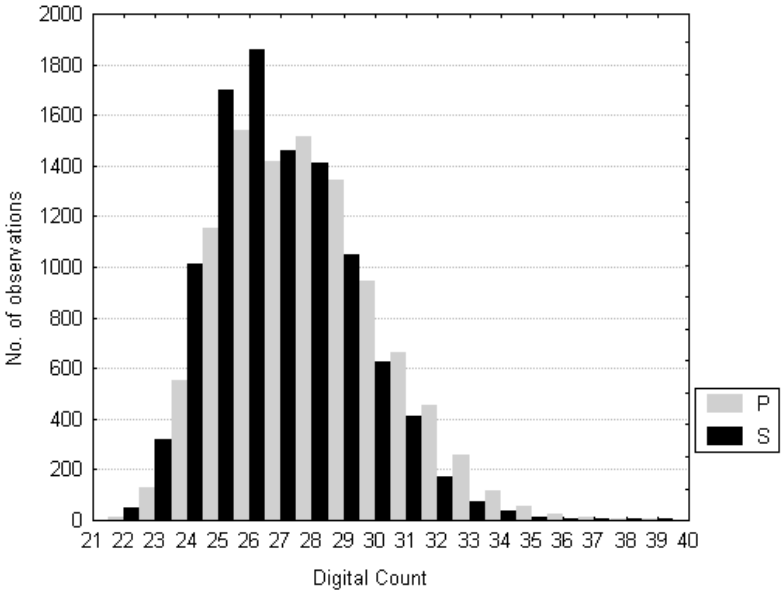

Figure 1: Sunlight source natural background data.

Some man-made target histograms are shown in Figure 2. They are separated due to a difference in polarization. However, they still show a Gaussian tendency.

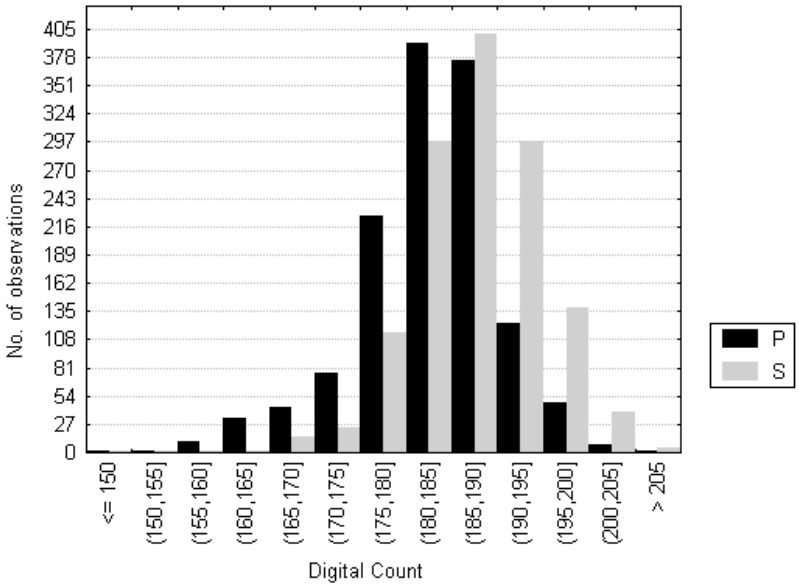

Figure 2: Man-made target response.

The detection algorithm, $F(\mathbf{X})$, was applied to several thousand samples from a variety of man-made targets on a grass background. The targets materials were various colors of metal and plastic. Some were easily visible in the grass while others blended with their background in color. The histograms for $F(P, S)$ and $F(P-S, P+S)$ are depicted together in Figure 3. A log scale is used for the detection values since $F(P, S)$ is an order of magnitude greater than $F(P-S, P+S)$.

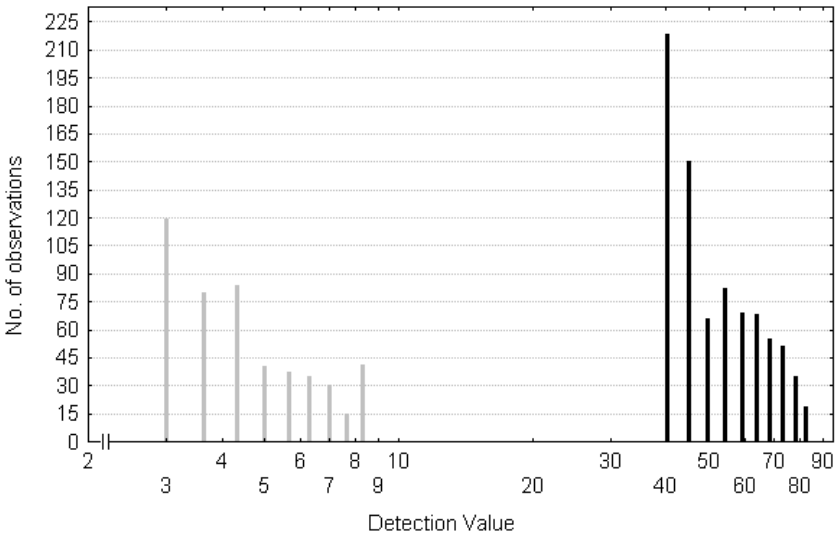

Figure 3: *F(P,S)* versus *F(P-S, P+S)*

The large separation between the detection values displayed in Figure 3 is due to an increased numerical sensitivity of $F(P-S, P+S)$ over $F(P, S)$. An important assumption was made in the false alarm rate comparison. That is the independence of reflectivity/emissivity and polarization. The independence is quantified by indicating $\text{cov}(P-S, P+S) = 0$. In reality, with the limited samples available in real imagery, numerically arriving at $\text{cov}(P-S, P+S) = 0$ is unlikely. In the samples, the background is often shades of a single color with slight variations of

a particular polarization property. This results in a strong correlation. This error term, e_c, is inserted into the covariance matrix as

$$\mathbf{S}_{P-S,P+S} = \begin{bmatrix} \mathrm{var}(P) + \mathrm{var}(S) & e_c \\ -2\,\mathrm{cov}(P,S) & \\ e_c & \mathrm{var}(P) + \mathrm{var}(S) \\ & +2\,\mathrm{cov}(P,S) \end{bmatrix}$$

The effect of this error term is create asymptotic behavior inverse of the matrix

$$F(P-S,P+S)_e = F(P-S,P+S)\left(\frac{\det(\mathbf{S}_{P-S,P+S})}{\det(\mathbf{S}_{P-S,P+S}) - e_c^2}\right) - \frac{2e_c(\mu_\mathbf{B} - \mu_\mathbf{T})_{P-S}(\mu_\mathbf{B} - \mu_\mathbf{T})_{P+S}}{\det(\mathbf{S}_{P-S,P+S}) - e_c^2}$$

The asymptotes are located at $e_c^2 = \det(\mathbf{S}_{P-S,P+S})$. Depending on the amount of error, the outcome could be significantly different than the theoretical value. This error chiefly affects the $F(P-S,P+S)$ result and experimental results showed that the covariance matrix using the directly measured images is not as susceptible to this type of error. This error could be artificially corrected in the computation of $F(P-S,P+S)$ by setting the off-diagonal elements of the covariance matrix to zero. By doing so, the result becomes comparable to $F(P,S)$. A dual histogram of the results is shown in Figure 4. Although the results are now comparable, the computation of $F(P-S,P+S)$ is artificial and not representative of the actual trends shown in the data.

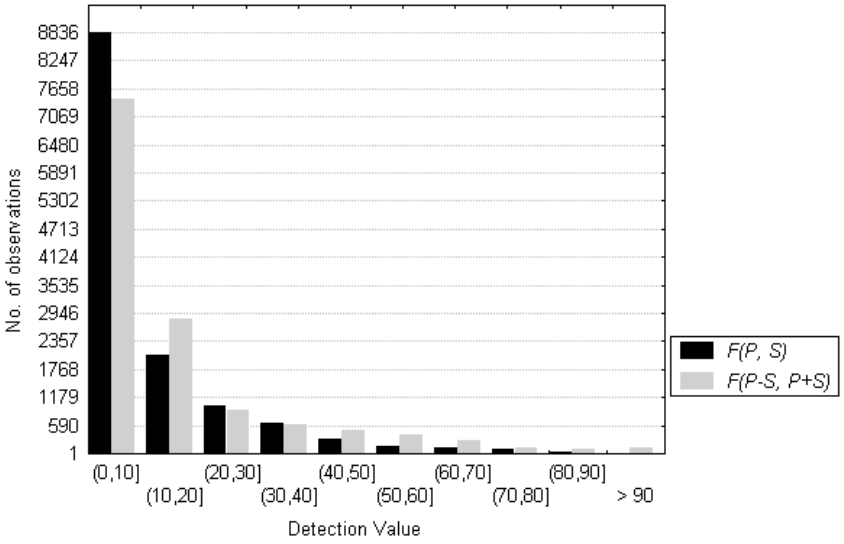

Figure 4: *F(P,S)* versus altered *F(P-S, P+S).*

6. CONCLUSION

Sometimes it is necessary to prove that polarization adds sufficient discrimination information. The polarization only and reflectivity/emissivity-only images are useful in proving the contribution of polarization in solving a particular problem. However, these Stokes images are not necessarily the best input into a detection algorithm. Once the utility of polarization has been shown, there may be no benefit to using the derived polarization and reflectivity/emissivity images in a detection algorithm.

This paper has shown that for a maximum likelihood ratio derived CFAR detection algorithm, combining the two directly measured images directly into a detection algorithm provides effective and efficient detection. Using the Stokes elements and the directly measured images produce consistent results. However, the Stokes imagery potentially introduces more

errors through its additional calibration calculations, and numerical sensitivity. Furthermore, when the background is depolarizing, the theoretical false alarm rate when using the directly measured images is no higher than that when the derived images are used. The example visible data actually shows it to be significantly lower. Although this result has only been proved for one type of detection algorithm, it certainly opens the question for other applications.

7. ACKNOWLEDGEMENTS

The author thanks the Office of Naval Research's Joint Mine Detection Technology program at the Coastal Systems Station in Panama City, Florida and U.S. Army Communications-Electronics Command Night Vision And Electronic Sensors Directorate's Lightweight Airborne Multispectral Minefield Detection program for providing insight and data.

REFERENCES

1. J. W. Williams, H. S. Tee, M. A. Poulter, "Image Processing and Classification for the UK Remote Minefield Detection System Infrared Polarimetric Camera", *Proceedings of SPIE Detection and Remediation Technologies for Mines and Minelike Targets VI* **4394**, 139-152 (2003).

2. Wim de Jong, Frank Cremer, Klamer Schutte, Jesper Strom, "Usage of Polarisation Features of landmines for improved Automatic Detection", *Proceedings of SPIE Detection and Remediation Technologies for Mines and Minelike Targets VI*, **4038**, 241-252 (2000).

3. Göran Forssell, "Passive IR Polarization Measurement Applied to covered Surface Landmines", *Proceedings of SPIE Detection and Remediation Technologies for Mines and Minelike Targets VIII*, **5089** 547-557 (2003).

[4]. Crosby, F. and S. Riley, "Signature Adaptive Mine Detection at a Constant False Alarm Rate", *Proceedings of SPIE Detection and Remediation Technologies for Mines and Minelike Targets* IV, April, 2001.

[5] William A Shurcliff,. and Ballard, Stanley S., *Polarized Light*, Van Nostrand, 1964.

[6] Taylor, J. S., et al. "Laboratory Characterization and Field Testing of the Tunable Filter Multispectral Camera", *Proceedings of SPIE Detection and Remediation Technologies for Mines and Minelike Targets VI*, **4394** 1247-1258 (2001).